Fractographic analysis of damage mechanisms dominated by delamination in composite laminates

A comprehensive review

Mohammadi, Reza; Assaad, Maher; Imran, Ahmed; Fotouhi, Mohammad

DOI
10.1016/j.polymertesting.2024.108441

Publication date
2024

Document Version
Final published version

Published in
Polymer Testing

Polymer Testing 134 (2024) 108441

Contents lists available at ScienceDirect

Polymer Testing

journal homepage: www.elsevier.com/locate/polytest

Fractographic analysis of damage mechanisms dominated by delamination in composite laminates: A comprehensive review

Reza Mohammadi [a,*], Maher Assaad [b], Ahmed Imran [c], Mohammad Fotouhi [a]

[a] Faculty of Civil Engineering and Geosciences, Delft University of Technology, 2628 CD, Delft, the Netherlands
[b] Department of Electrical and Computer Engineering, College of Engineering and IT, Ajman University, Ajman, P.O. Box 346, United Arab Emirates
[c] Department of Biomedical Engineering, College of Engineering and IT, Ajman University, Ajman, P.O. Box 346, United Arab Emirates

ARTICLE INFO

Keywords:
Composite laminates
Delamination-dominated damages
Fractography analysis
SEM analysis
Review paper

ABSTRACT

Polymer composite laminates have established themselves as essential materials across a wide type of industrial fields because of their specific mechanical properties such as high strength and low weight. Among the main issues they face is susceptibility to delamination damage. This comprehensive review paper investigates various damage mechanisms and associated phenomena that obvious during delamination within polymer composite laminates. Delamination can primarily arise in Mode I, Mode II and mixed Mode I &II loading scenarios. Notably, the damage features can vary significantly between these conditions. This paper aims to characterize and identify delamination-dominated damage features by conducting a comprehensive examination of the parameters that influence these features, all based on an extensive literature review and utilizing fractography analysis. The findings of this review illustrate the valuable insights that can be obtained from delamination fracture surfaces through the utilization of fractography images and the examination of damage features. For instance, it is possible to recognize details such as determining of global crack growth direction, calculating the rate of fatigue crack growth, and anticipating of strain energy released rate. This deeper understanding aids in pinpointing the key factors contributing to delamination damage. It could offer valuable insights for designing composites resistant to delamination. Additionally, it may assist in determining the underlying causes of catastrophic failures in tragic events.

1. Introduction

Nowadays, composite materials have obtained significant traction in a different industrial fields such as petrochemical, aerospace, automotive, and civil engineering. Composites primarily consist of two key components: fiber and resin. These reinforcing fibers can include various materials like carbon, glass, Kevlar, and others, while the matrix resin can be different polymers including polyester, vinyl ester and epoxy. The benefits of composite laminates include their high strength, low weight, resistant to chemical corrosion, design flexibility and user-friendly manufacturing processes [1–6]. Despite these benefits, composite laminates can still experience various damage mechanisms due to their inherent structures, resulting from the manufactured combination of matrix and reinforcement [7–11]. Delamination is a frequently observed mode of failure that often initiates from cracks within the material, resulting in fracture and the ultimate failure of structures [12–15]. In recent decades, significant research efforts [16–20] have been directed towards investigating the delamination behavior of composite laminates. Some of this studies [21–26] have involved conducting fractography analyses, often utilizing Scanning Electron Microscopy (SEM) to consider fracture surface of delamination in greater detail and understand the underlying damage mechanisms.

It is imperative to acknowledge the existence of three primary damage mechanisms namely, fiber breakage, matrix cracking, and fiber-matrix debonding, which are commonly visible on the fracture surface of delamination. Moreover, these damage mechanisms give rise to distinct damage features on the interlaminar fracture surface. An example of such a feature is the cusp, a unique form of matrix cracking that emerges as a consequence of the stress conditions at the fracture surface. Additionally, there exist various other features, such as scarp, riverine, striation, roller cusps, and hackle patterns will be thoroughly explored in the following sections of this paper. These damage mechanisms manifest at various length scales, ranging from the microscopic level (illustrated by phenomena such as scarp and striation) to the less discernible scale of

* Corresponding author.
E-mail address: rezam75@gmail.com (R. Mohammadi).

https://doi.org/10.1016/j.polymertesting.2024.108441
Received 10 February 2024; Received in revised form 24 March 2024; Accepted 2 May 2024
Available online 3 May 2024

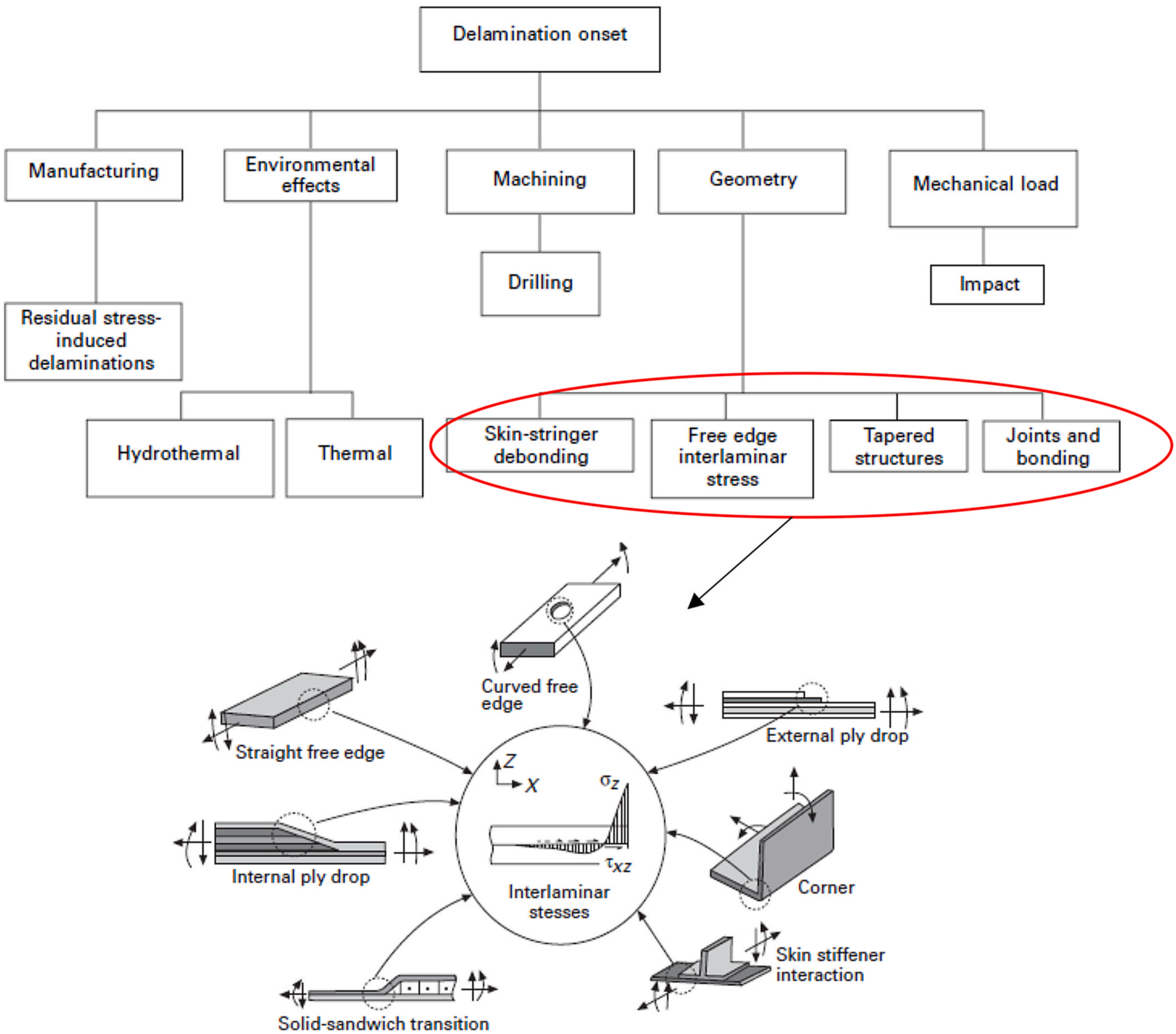

Fig. 1. Delamination source in composite laminates [32].

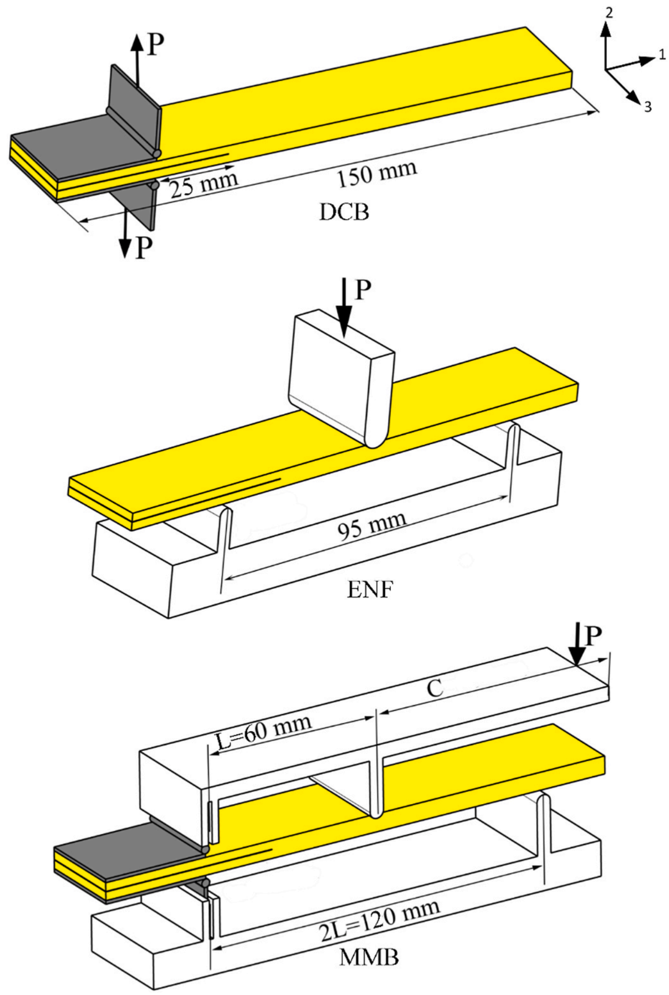

Fig. 2. The schematic test setup of DCB (mode I), ENF(mode II) and MMB (mixed mode I&II) specimens [40].

fiber/matrix debonding, and finally, to the macroscopic level, which is readily observable and includes matrix cracking and delamination.

This research paper focuses on characterizing and identifying damage features associated with delamination. To achieve this, fractography analysis was utilized, integrating findings from an extensive literature review and SEM images captured by authors. This approach has allowed for the presentation of a detailed overview of the various features arising from the damage mechanisms. Fractography analysis in composite laminates provides valuable insights for both the repair and design of composite structures. Analyzing damage features and recognizing damage mechanisms in composite laminates, it becomes feasible to gain insights to design delamination-resistant composites as well as identify the root causes of catastrophic failures in tragic incidents. For instance, as it can be seen in this paper, through these techniques and the inspection of fracture surfaces, it is possible to estimate the crack propagation direction, calculating of fatigue crack growth rate, and determining of Strain Energy Release Rate (SERR), consequently shedding light on the level of load applied on the structure. This review paper has been characterize to 8 sections as follow: 1- introduction, 2- The origins of delamination 3- Resin-rich area 4- Fiber bridging phenomena 5- Fiber breakage 6- Fiber/matrix debonding 7- Matrix cracking 8- Conclusion. In Section 7, an extensive review has been conducted on the various types of matrix cracking features, which are discussed in the following subsections: 7-1- Revealing delamination orientation via cusps, 7-2- Roller cusps, 7-3- Scarp features 7-4- Striations indicating the fatigue crack growth rate, 7-5- Fracture surface as an indication of the energy release rate.

2. The origins of delamination

Delamination is known as interface crack occurring between two adjacent layers in composite laminates [27]. Delamination can originate from various sources, including impacts [28], manufacturing imperfections during cutting and drilling process [29,30], and stress concentrations resulting from structural changes [31]. The primary origins of this interlaminar cracks are associated with composite materials inconsistencies, which generate interlaminar stresses. Delamination typically appears at free edges because of incompatibility in the mechanical properties of adjacent layers, at ply transitions where thickness reductions are necessary, and in areas subjected to out-of-plane bending loads.

As per Fig. 1, delamination in composite structures can be attributed to various factors, including mechanical load, geometry, machining processes like drilling, environmental effects (thermal and hydrothermal), and manufacturing processes. Additionally, delamination may be induced by geometric factors such as free edges, joints, stringers and taper due to the free edge effect. The free edge effect occurs from differences in the elastic constants of adjacent layers, resulting in the development of stress concentrations near the free edge and at the interfaces between layers. Many researchers tend to categorize delamination into distinct pure modes including, Mode I (peel), Mode II (shear) and Mode III (tear). Among these, modes I and II, or a combination of both, are more frequently studied. This focus is due to the relatively rare occurrence of mode III delamination due to the higher strain energy level requirement.

One prevalent instance of delamination in composite laminates arises from impact events, often leading to barely visible impact damage (BVID). BVID has the potential to significantly reduce strength without apparent warning. Structures appearing undamaged may experience sudden failure at loads considerably lower than anticipated [28,33–35].

2.1. Mechanical characterization methods

To assess the delamination behavior of composite laminates, including factors like interlaminar fracture toughness (G_{IC}, G_{IIC}) and crack growth rate, ASTM standards have been established. Accordingly, ASTM D 5528 [36], ASTM D7905 [37], and ASTM D6671 [38] have been developed for Mode I, Mode II, and Mixed Mode I & II, respectively. Additionally, ASTM D6115 [39] is employed to study of delamination growth onset under Mode I fatigue loading. Consequently, our research focuses on analyzing delamination-dominated damage mechanisms through fractography analysis under static and fatigue conditions in mode I, mode II, and mixed mode I & II. Researchers typically conducted these tests following established standard guidelines. Fig. 2 illustrates the schematic of fracture tests on composite specimens in three different modes.

In the upcoming sections, we will explore prevalent damage phenomena, damage mechanisms, and damage features that may appear during delamination, as analyzed through the fractography method. Fig. 3 shows the schematic summary of delamination-dominated damage mechanisms and related features.

3. Resin-rich area

Resin-rich regions, also known as resin-rich zones, frequently occur composite structures, exerting a considerable influence on the material properties and the onset of damage [41]. These areas denote portions of the matrix material that exhibit localized richness in resin, resulting in a corresponding deficiency of fibers. Researchers utilize resin-rich areas as vital indicators to assess various properties of the composite laminates, including tensile or compression strength [42], fracture toughness [43], strain to failure [44] and volume resistivity [45].

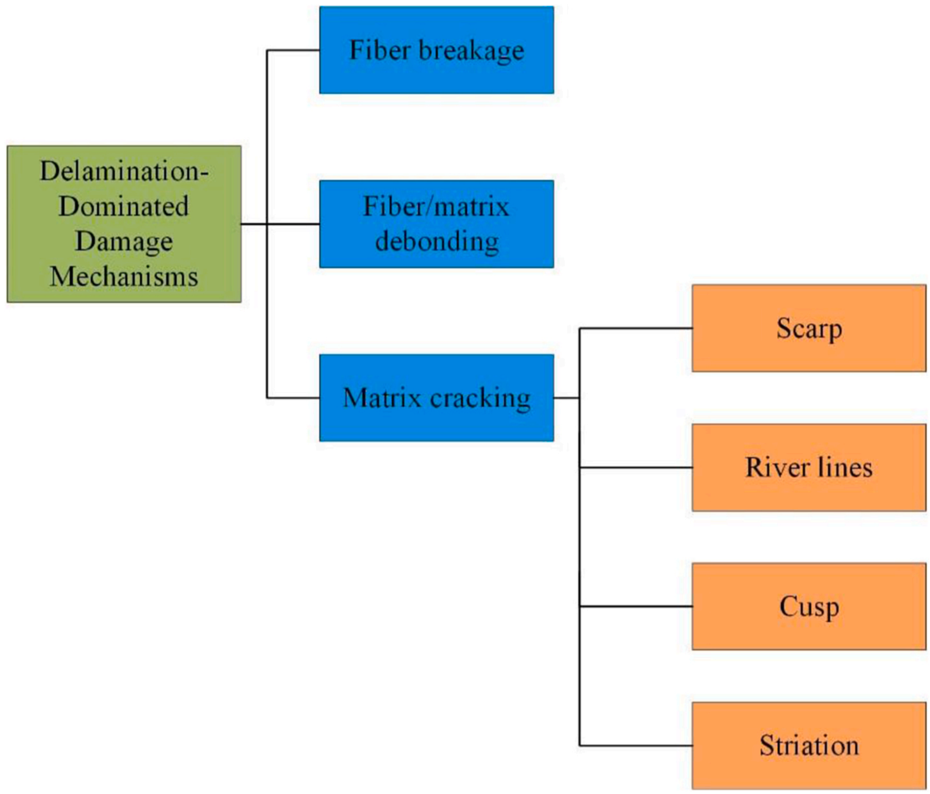

Fig. 3. Dominant delamination damage mechanisms and associated features in composite laminates.

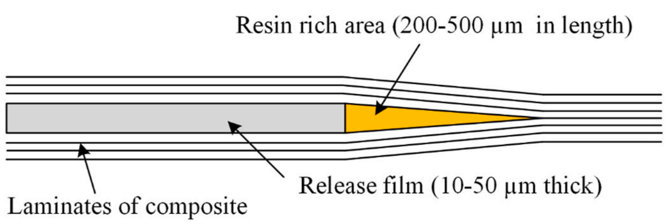

Fig. 4. The exaggerated schematic of resin rich area in composite laminate.

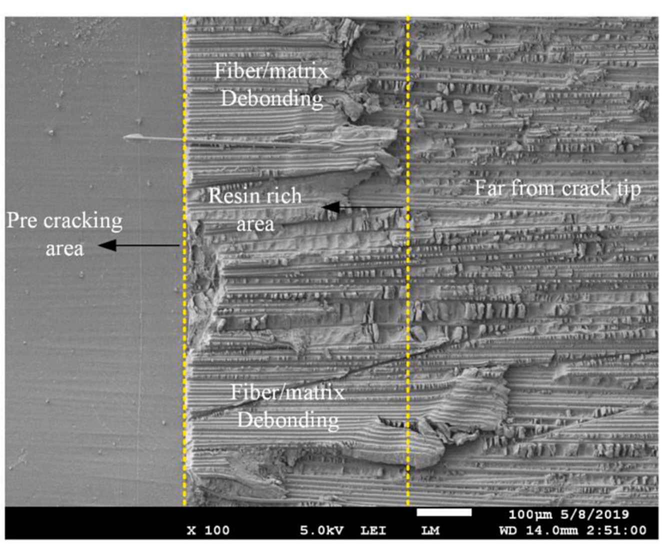

Fig. 5. Resin-enriched zone near the initial crack tip under static mode II loading condition [47].

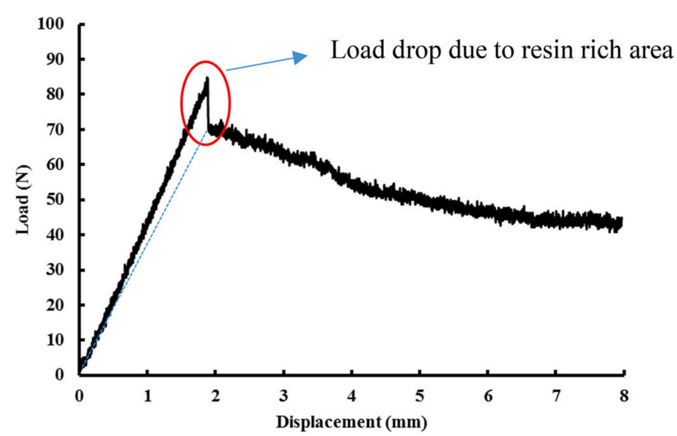

Fig. 6. The influence of resin rich area on load displacement curve on mode I loading condition for AS4/8552 materials [50].

In interlaminar fracture test specimens, a resin-rich region is typically formed due to the presence of pre-crack initiators, such as PTFE (Polytetrafluoroethylene) film. Complying with standard guidelines such as ASTM D5528 [36], ASTM D6115 [39] and ASTM D7905 [37], a thin release film, is interposed between the middle of layers to induce an initial crack. This film typically has a thickness of 10–50 μm [46], resulting in the formation of a triangular region characterized by an excess of resin, as shown by Fig. 4. Furthermore, Fig. 5 illustrates the SEM micrograph of the resin-rich area at the crack tip under mode II static loading conditions.

Moreover, the presence of a resin-rich region can impact both the load-displacement graph, as illustrated by Fig. 6, and the fracture toughness values. Some research investigations have been conducted to analyze the effects of release film and pre-cracks on G_{IC} values [48,49].

Fig. 7 illustrates a representative set of results, showcasing increased

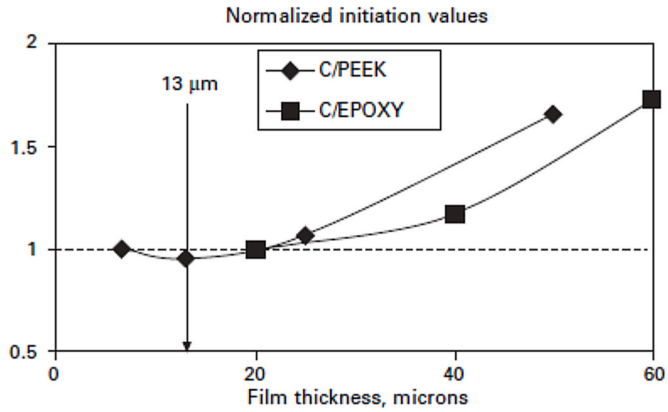

Fig. 7. The influence of release film thickness on fracture toughness carbon/epoxy and carbon/PEEK unidirectional composite laminates [32].

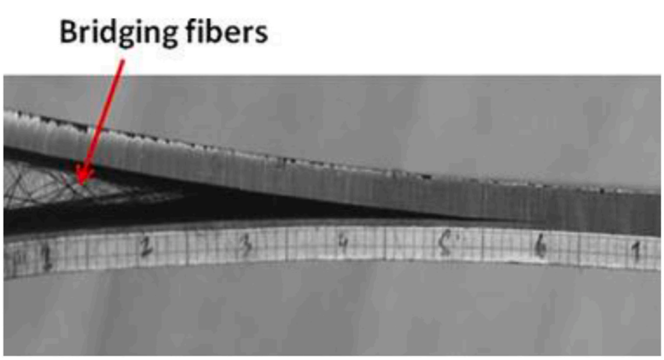

Fig. 8. Fiber bridging phenomena in mode I test specimen [51].

fracture toughness values when thicker films are utilized. This behavior is primarily linked to the resin-rich region near the film. Based on the graph, it is observed that at a thickness of 13 µm, the resin-rich area has the least impact on fracture toughness (G_{IC}) values. Consequently, the standard recommends adopting the same value for this reason.

4. Fiber bridging phenomena

In fiber bridging phenomenon, the fibers bridge between two adjacent layers and act as crack arrestors due to which the delamination resistance and fracture toughness increases [51]. Fiber bridging can occur in mode I, Mode II, and mixed mode I & II, but it is a common phenomenon in mode I as depicted in Fig. 8. In unidirectional laminates, fiber bridging tends to develop rapidly, and while reducing the relative angle between adjacent plies can mitigate the extent of bridging, but it does not entirely eliminate it. Conversely, within woven fabric laminates, there is a possibility of fiber bridging, but the extent of bridging is generally minimal. As seen in Fig. 9 fiber bridging is more prevalent in unidirectional laminates as opposed to woven ones.

Fiber bridging demonstrates potential in improving the mechanical properties of both inter-laminar and in-plane aspects in composite laminates. Put more simply, this phenomenon elevates the interlaminar fracture toughness of the specimen from its initial G_{IC} value to higher levels [52,53]. The presence of fiber bridging ensures stable crack growth between laminates [54]. In recent decades, researchers have conducted extensive studies on fiber bridging. They have considered different aspects of the fiber bridging phenomenon, including bridging laws, origin of bridging, the impact of bridging on fracture toughness and R-curve, and variations in bridging under static and fatigue test [55–60].

In quasi-static delamination tests, fiber bridging significantly

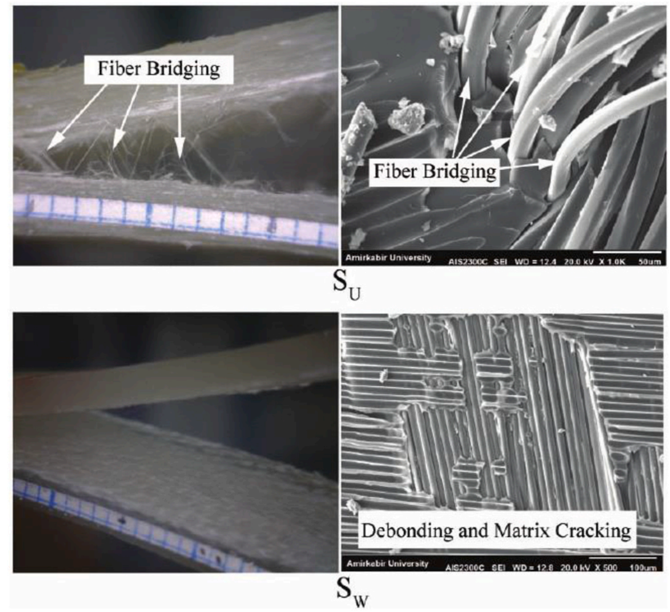

Fig. 9. Fiber bridging is more prevalent in unidirectional GFRP laminates as opposed to woven ones [12].

increases fracture toughness [51,61–65]. Furthermore, in fatigue testing, the occurrence of fiber bridging can exert a notable influence on the fatigue behavior and related constants of Paris law. This effect is evident in Fig. 10, where the fatigue curves shift significantly from left to right as the length of the fatigue pre-cracks increases, indicating the development of fiber bridging. This shift implies that the Strain Energy Release Rate (SERR) required for a specific crack growth rate (da/dN) is not constant but relies on the extent of crack extension ($a-a_0$), which is a measure of the degree of fiber bridging. As the crack extends, more bridging fibers can accumulate in the wake of the crack front, leading to the cyclic storage and release of additional strain energy within them. Consequently, this artificially contributes to a higher value of SERR.

5. Fiber breakage

Fiber breakage represents a common damage mechanism identified in the fracture surface of delamination during fractography analysis. This typically involves the phenomenon of fiber bridging between layers, frequently followed by fiber breakage. When the stress applied to these bridged fibers surpasses their strength, the fibers fracture, causing a sudden crack propagation over a short distance. Subsequently, the crack is re-arrested by the bridging action of new fibers [66]. In these scenarios, clusters and groups of fibers often experience breakage. Fig. 11 depicts an example of fiber breakage occurring in groups due to fiber bridging in the mode-I fracture surface of a CFRP laminate. As a result of the group breakage of fibers, there is typically a sudden decrease in load-displacement diagram.

In Fig. 12, the crack growth-displacement and load-displacement graphs for unidirectional glass/epoxy under quasi-static Mode I loading are presented. Significantly, the load-displacement curve exhibits instabilities marked by fluctuating patterns, commonly known as the pop-in phenomenon [54]. These load drops result from the group failure of bridged fibers. As fibers bridge between the upper and lower layers, they experience tensile stress. As the tension force in the fibers gradually rises, reaching the breaking stress, the bridged fibers fracture, leading to sudden crack growth. This abrupt increase in crack length results in a sudden drop in load (pop-in) [68,69]. Subsequently, create of new bridging fibers arrests the crack once again. It is important to note that the first pop-in, in Fig. 12 is associated with a resin-rich area. Additionally, with each load pop-in, there is an abrupt extension of the

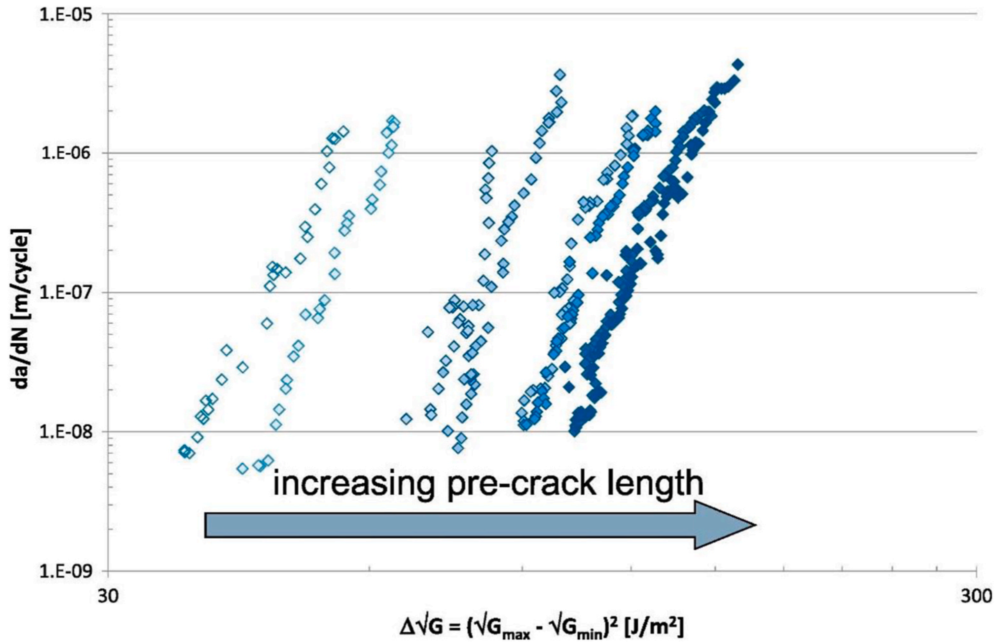

Fig. 10. Fatigue resistance curves: Exploring the influence of Pre-crack length emphasizing the impact of fiber bridging [60].

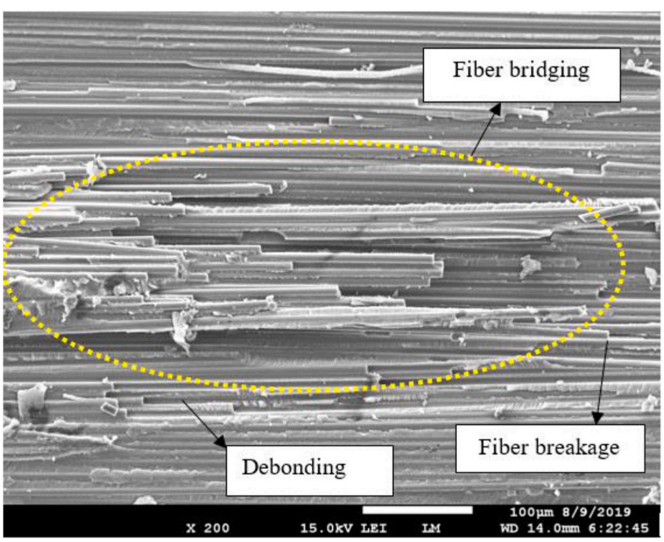

Fig. 11. Micrograph illustrating group fiber breakage resulting from fiber bridging [67].

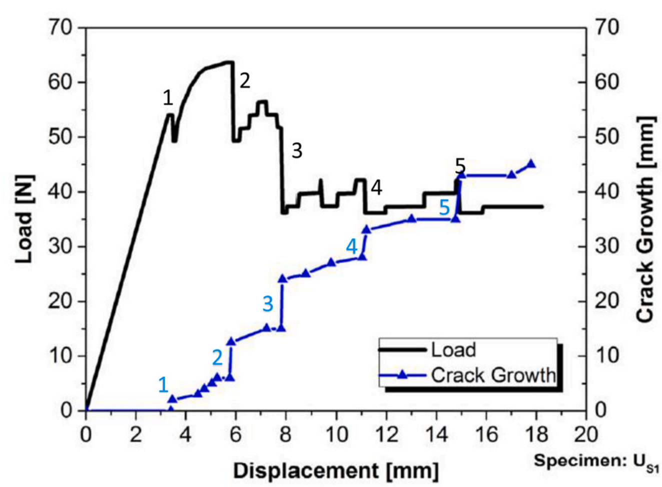

Fig. 12. Considering of fiber bridging effect on load-displacement and crack growth behavior [66].

crack length by a few millimeters.

6. Fiber/matrix debonding

Another main damage mechanism in composite laminates is the debonding between matrix and fibers, typically initiated by a perpendicular load applied in the direction of the fibers. In Fig. 13(a)–a simplified depiction illustrates the basic structure of a 0/90/0 laminate, showcasing the occurrence of fiber/matrix debonding. Moreover, the coalescence of these deboned areas can lead to the creation of a big crack (Fig. 13 (b)).

The fiber-matrix debonding, is significantly related to strain amplification within the matrix located between two adjacent fibers. The amplification of strain arises from the inherent difference in Young's modulus between the fibers and the matrix.

In delamination fracture surfaces, the presence of fiber-matrix debonding is identified through the appearance of fiber or fiber imprints in matrix, indicating the occurrence of bonding between the fiber and matrix. Fig. 14 presents SEM findings regarding fracture surfaces in a quasi-static test of a multidirectional composite laminate. It is evident that the predominant microscopic feature on the top surface of the fractures is the imprint of fibers. Conversely, the opposite surface exhibits naked fibers that appear exceptionally smooth and free from any matrix residue or bonding. This observation underscores the importance of the fiber/matrix interfacial strength in the delamination of such composite materials.

The behavior of a fiber-reinforced composite is notably shaped by the attributes of the interface between the fiber and the matrix resin. The adhesive bond at the interfacial surface plays a pivotal role in influencing the overall mechanical properties of the composite. This interface is essential for effective stress transfer between the fiber and matrix. In scenarios where the fibers have a weak connection with the matrix, the composite initiates matrix cracking at a relatively low stress level. Conversely, with strong bonding between fibers and the matrix, matrix

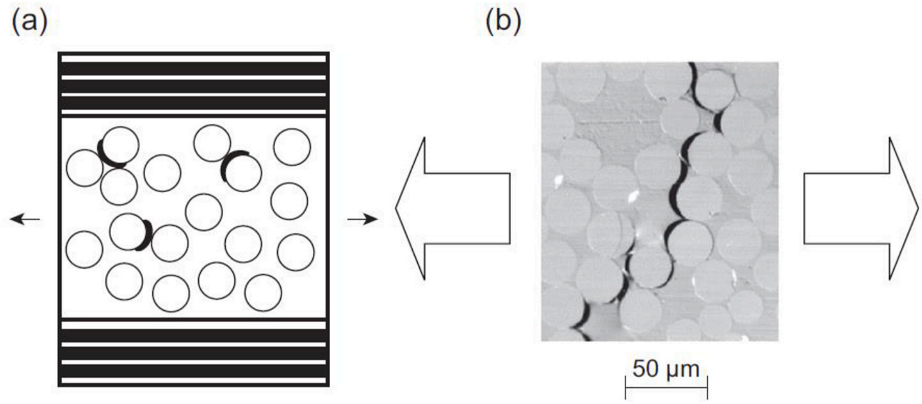

Fig. 13. **A)** Fiber-matrix debonding in 0/90/0 cross ply **B)** a big crack has been created due to coalescence of fiber matrix debonding [70].

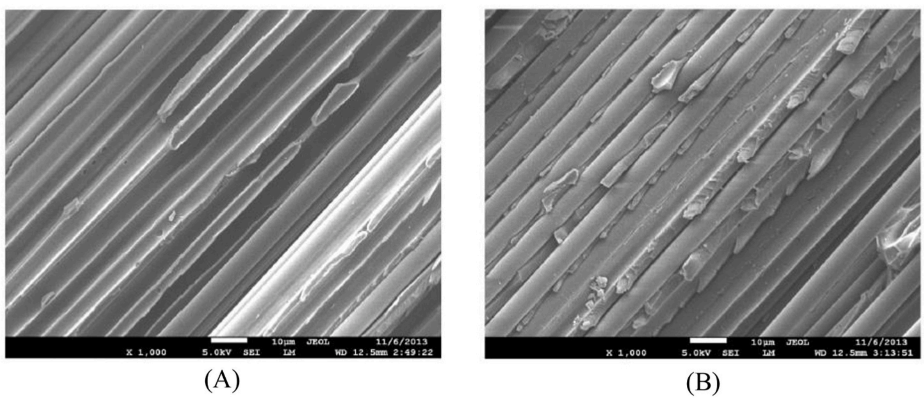

Fig. 14. Fractographic images of mode-I fracture surfaces **A)** Fiber imprints on top surface **B)** Fibers on down surface [71].

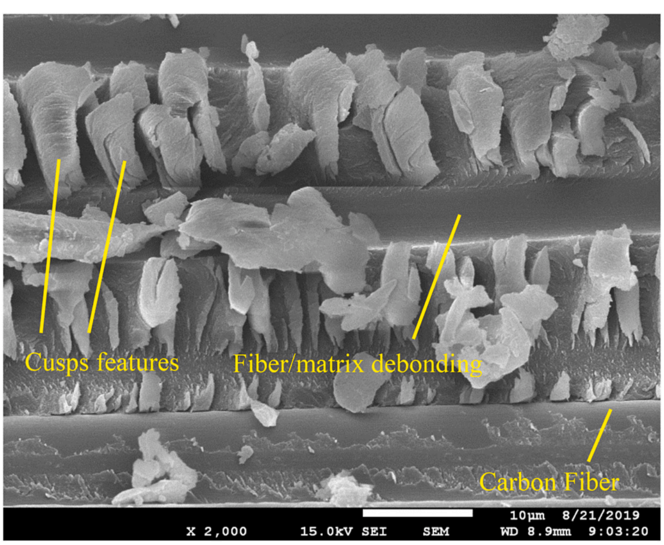

Fig. 15. Formation of cusp from matrix cracking [78].

cracking is postponed, leading to catastrophic failure due to fiber fracture when the matrix eventually cracks.

7. Matrix cracking

Matrix cracking is another primary damage mechanisms which commonly observed in composite materials [72]. Due to the inherent structural makeup of composite laminates, comprising both matrix and reinforcement, any kind of macro damage that occurs in the structure is associated with matrix cracking. For example, the delamination between the layers, which is considered a macro damage, does not happen unless the matrix cracking has happened before that while there is a possibility that no fibers break during crack propagation. For example, analyzing fractography of fracture surface under mode II loading conditions reveals that fiber breakage is infrequently observed. Typically, under this loading condition, observable occurrences include fiber-matrix debonding and matrix cracking. Moreover, in theory, when there exists a robust connection between the fiber and the matrix, the mechanism of fiber-matrix debonding may not be apparent, while the mechanism of matrix cracking remains observable. Therefore, delamination is always accompanied by matrix cracking. By examining the fracture surfaces of the delamination, the mechanisms of matrix cracking are shown as different type of features according to different type of loading condition (static, fatigue, loading rate, etc.). The subsequent sections consider a thorough examination of the different type of matrix cracking features, exploring their characteristics in-depth.

7.1. Revealing delamination orientation via cusps

One of the key fractography features on delamination fracture surfaces is the presence of cusps, which manifest as raised platelets [73–75]. This feature also called Hackle by some researchers [76,77]. The inclination of these cusps can serve as a valuable indicator for discerning local shearing directions on the surfaces. Fig. 15 illustrates a cusp that formed from matrix cracking in CFRP laminates. To effectively utilize these features, it's essential to control the lighting conditions to cast shadows from the cusps, enabling the determination of their tilt

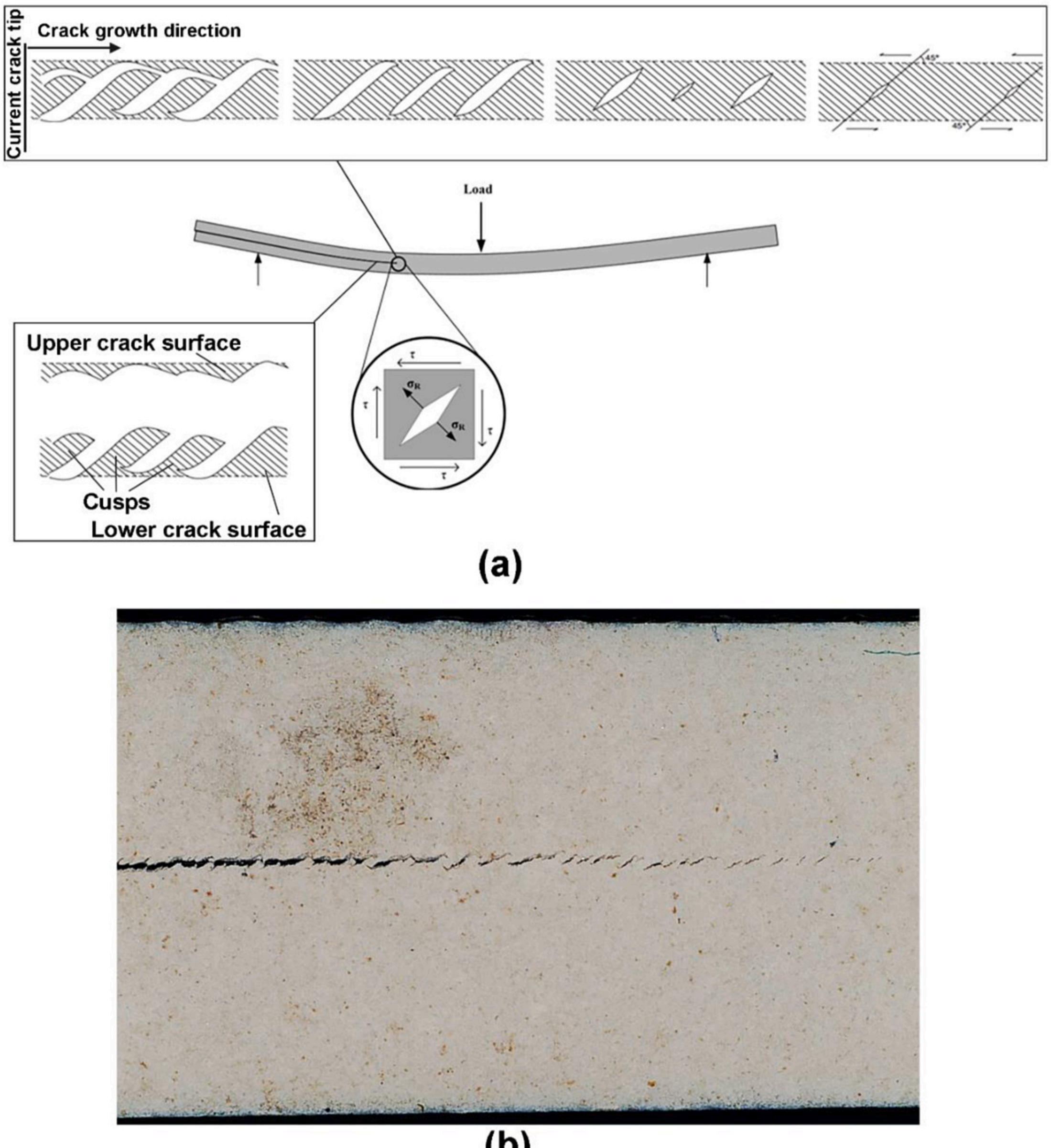

Fig. 16. Formation of Cusps under Mode II Loading: a) Schematic and b) Actual Side View of ENF Specimen [79].

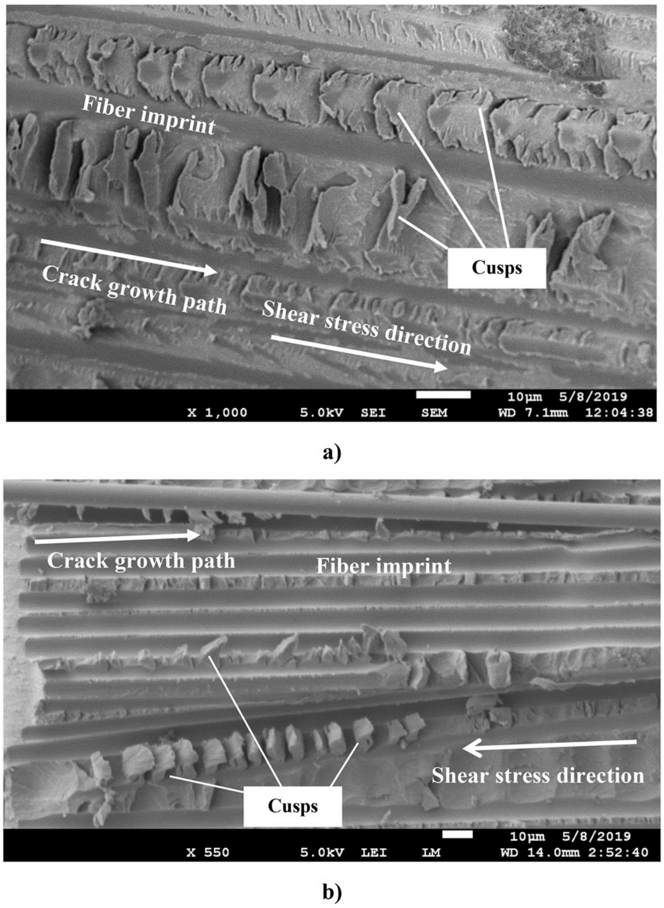

Fig. 17. Determining of delamination orientation via cusps in mode II loading of CFRP materials: **a)** The SEM micrograph of upper fracture surface **b)** The SEM micrograph of lower surface [79].

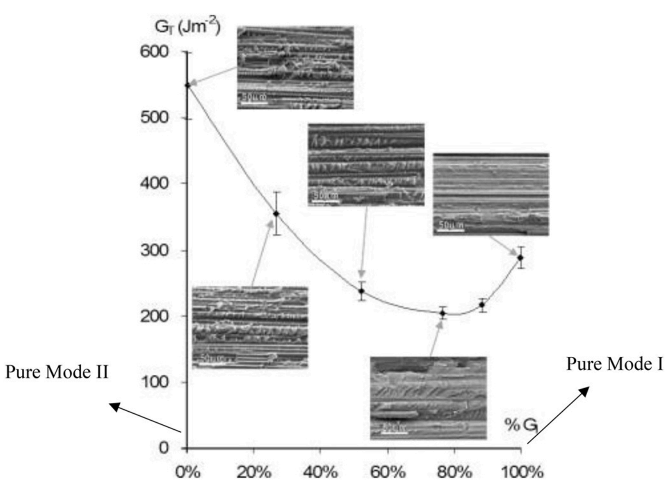

Fig. 18. Fracture surface morphology and cusp Percentage as criteria for determining mixed mode ratio and fracture toughness [80].

direction. Given their potential small size, it's advisable to focus on larger cusps, particularly in regions with a higher resin fraction, as they facilitate a clearer deduction of the tilt direction. Moreover, examining the corresponding fracture surface can aid in resolving any complex areas and validating the primary surface observations.

Fig. 16 provides a schematic representation of the cusp formation procedure during mode II test. As depicted, the stress state at the crack

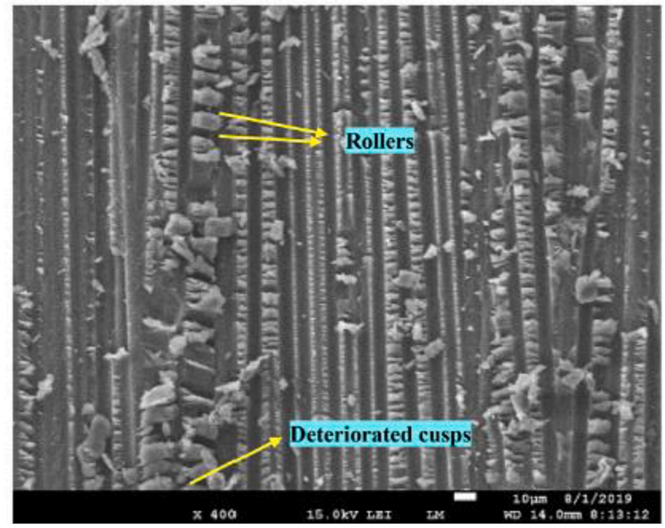

Fig. 19. Fractography analysis of fracture surface of AS4/8552 laminates on mode II fatigue test [47].

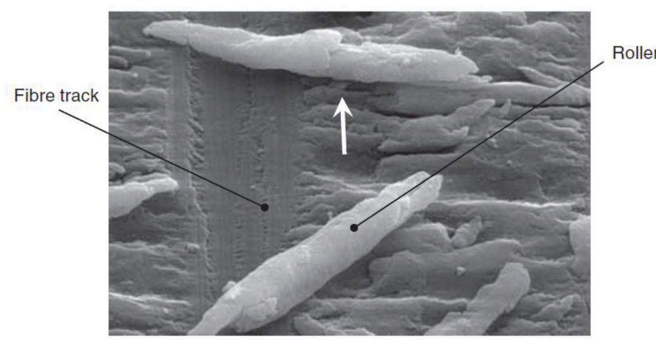

Fig. 20. Fractographic Analysis of the Fracture Surface of HTA/6376 Laminates subjected to mode II fatigue test (X17000) [82].

front induces angular matrix cracks at a 45-degree angle. With gradual enhancing loads, angular cracks grow and coalesce to give rise to cusps. For a more precise analysis, selected sites should undergo electron microscopy to corroborate optical observations of the cusps. The orientation of these cusps can provide insight into the overall direction of crack growth, as cusps typically develop in opposition to the shear stress direction.

For instance, the shear stress direction corresponds to the crack growth on the upper fracture surface (Fig. 17-a), whereas, it runs counter to the crack growth direction on the opposite fracture surface (Fig. 17-b). As a result, cusps on the lower surface align with the crack growth direction, while those on the upper surface form in opposition to it.

Another noteworthy aspect to highlight is the difference observed in fracture surfaces under mode I and mode II loading conditions. In mode I loading, the fracture surface tends to be smoother with cleavage matrix cracking, typically resulting in lower fracture toughness compared to mode II. However, under mixed mode I & II loading conditions, an increase in the percentage of mode II loading leads to a rougher fracture surface due to the formation of cusp features, consequently enhancing toughness. The formation of cusps increases compliance and makes the structure more ductile. Hence, the presence of cusps on the fracture surface serves as a criterion for determining the ratio of mode I to mode II loading in mixed mode conditions and for evaluating total fracture toughness. Fig. 18 illustrates the correlation between the presence of cusps on the fracture surface, mixed mode ratio, and total fracture

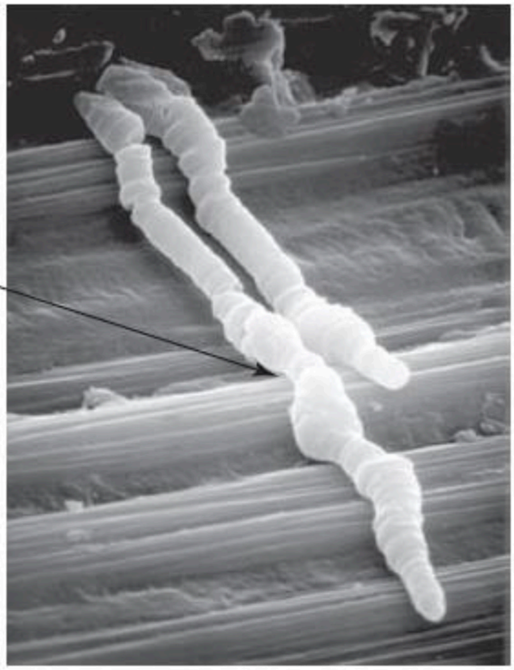

Fig. 21. Matrix rollers of T300/V390 composite materials (X4000) [83].

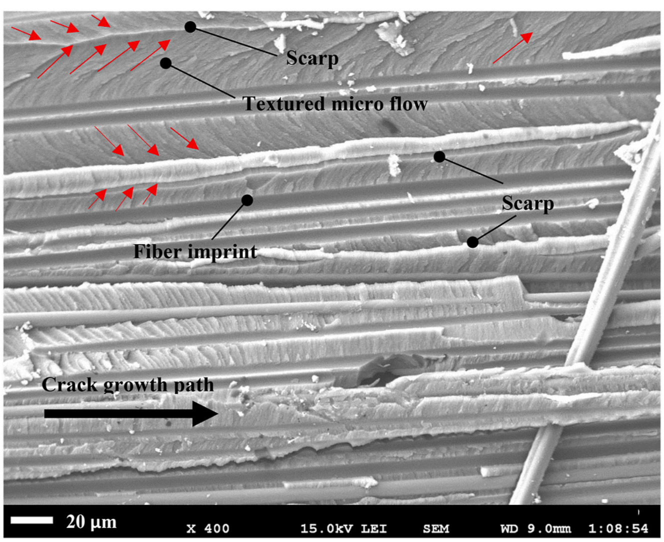

Fig. 22. Formation of scarp lines in mode I CFRP laminates [50].

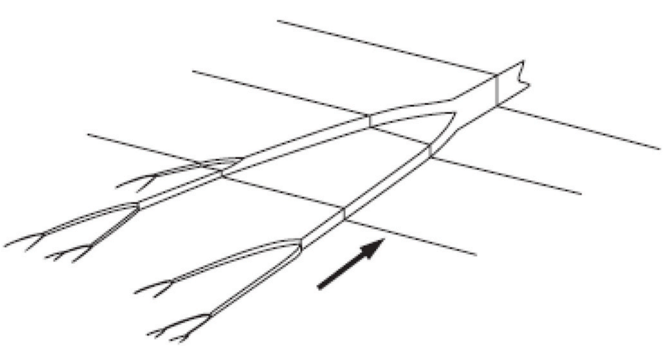

Fig. 23. Spread of river-line features [84].

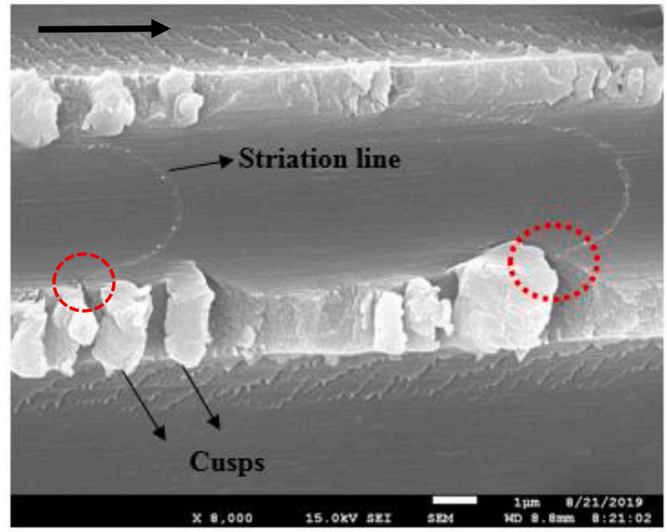

Fig. 24. Formation of fatigue striation lines adjacent to the cusp features in mode II CFRP laminates (x8000).

toughness.

7.2. Roller cusps

Another interesting occurrence during mode II fatigue loading is the transformation of the cusps into cylindrical shapes. This phenomenon is a consequence of the cyclic movement of two surfaces (up and down) in opposing directions, causing the cusps to undergo a transformation into worm-like structures oriented perpendicular to the fiber direction. Additionally, under these loading conditions, some of the cusps become crushed and deteriorated, scattering fragments across the surface. Fig. 19 displays the fracture surface of the CFRP laminate under fatigue loading, with visible cusp rollers (highlighted as rollers). The size of these cusps depends on the fracture toughness of the resin, greater resin toughness results in longer cylinder lengths. Accordingly thermoplastic matrix resins will exhibit roller cusps with more length. A closer inspection of these cylinders reveals that they demonstrate substantial plasticity, even within brittle matrix polymers, and may separate from the fracture surfaces (refer to Fig. 20). The presence of plasticity in this context may be attributed to the conditions of mode II fatigue test. In this scenario, the local temperature on the fracture surface rises, primarily due to heat generated from friction between the two surfaces and hysteresis loops resulting from the cyclic loading [81]. Consequently, the brittle matrix can display plasticity behavior as the temperature nears its glass transition temperature (T_g).

In Fig. 21, the micrograph surfaces of T300/V390 can be observed. Notably, the matrix rollers are clearly visible and display a remarkable level of ductility, which is quite surprising, especially considering that this material is a brittle bismaleimide polymer. Additionally, with more detail consider of matrix roller surface, imprint of the underlying fibers is noticeable on the surface [83].

7.3. Scarp features

The occurrence of a scarp represents a fascinating and significant phenomenon when examining the failure surfaces of polymer composites. These features typically apparent as relatively bright lines in microscopic images, aligned with the direction of the fibers. The scarp lines form as a result of the convergence of two neighboring crack planes [84]. The process through which scarp lines develop involves an initial localized failure at high risk points, such as interface of matrix and fiber [85]. This localized failure triggers the propagation of microcracks

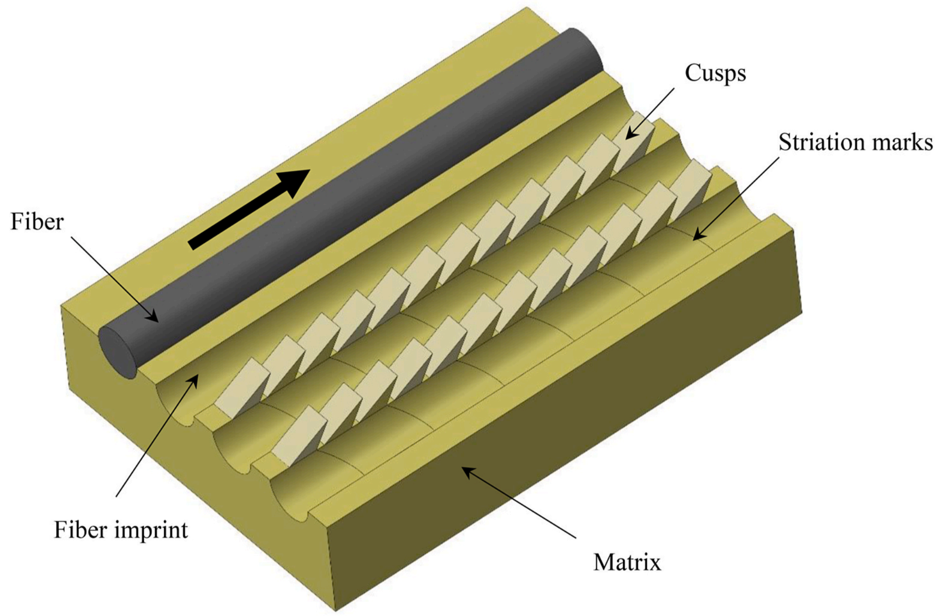

Fig. 25. A schematic representation of the formation of striations and cusps during the fatigue delamination process.

within both the matrix and around the fiber. Initially, these cracks begin to propagate at a 90-degree angle to the fiber direction. However, since the primary crack's trajectory aligns with the fiber direction, these microcracks gradually reorient themselves towards the global crack growth direction. Ultimately, the matrix microcracks may spread as microflow on several different planes and, as they converge, they coalesce into a distinct line, forming what is known as a scarp. Fig. 22 shows the scarp features which are created during the mode I loading condition in CFRP laminates. As shown in this figure, microcracks in the matrix initiate at fiber intersections and extend as textured microflows, following the primary direction of crack growth within the matrix and at the intersections of the scarps. This phenomenon gives rise to the distinctive sharpness observed. Furthermore, the alignment of textured micro flow lines within matrix microcracks serves as a valuable indicator for predicting the path of the global delamination propagation.

To determine the primary crack direction from fractography images using the scarp lines, the initial step is to identify the scarp line. Subsequently, by considering the propagate direction of microcracks from both sides toward the scarp lines (as denoted by the red arrows in Fig. 22), it can be establish the overall crack direction. This method offers an advantage over the previously mentioned cusp approach in that it doesn't depend on assessing the elevations (upper or lower fracture surface) to determine the main crack path. Actually, this methodology enables the recognition of the crack growth direction, regardless of whether the image corresponds to the upper or lower fracture surface. The way matrix microcracks grow and spread can be like a river stream. In such a way that the matrix microcracks in one plane from different branches have reached each other and form a bigger crack. This phenomenon can also be called river lines. For a more accurate interpretation of this phenomenon, see Fig. 23.

7.4. Striations indicate the fatigue crack growth rate

Another notable characteristic observed on the fracture surface of specimens subjected to fatigue testing, typically observable in high-magnification SEM images, is the existence of striation marks. These striations represent distinctive markings etched onto the fatigue surface, revealing the step-by-step progression of the fatigue crack. Furthermore, they indicate location of the crack tip at the time of its formation. Striation lines created due to the fracture of molecular chains at the tip of the crack, taking place following a limited amount of tension [76,79,84]. Fig. 24 displays the development of fatigue striation lines near the cusp features in Mode II fatigue tests for CFRP laminates (AS4/8552 Hexcel Prepreg). These images were captured by the authors of this article. To produce this photograph, carbon/epoxy samples measuring 180 *25 *4.5 mm^3 were prepared. An initial pre-crack was induced in the samples, followed by subjecting them to mode II fatigue loading as per standard ASTM D7905. The specimens underwent sinusoidal cyclic loading at a frequency of 3 Hz with a cyclic loading ratio of $R = 0.3$. Further methodological details were presented in Ref. [47]. For better understanding, Fig. 25 illustrates a schematic depiction of the formation of striations and cusps throughout the fatigue delamination process.

It has been reported that each individual striation corresponds to one cycle of fatigue [86].

In this case, the distance between each pair of neighboring striation marks acts as a gauge of the fatigue crack growth rate at that particular instant. An illustrative instant of this relationship is provided in Ref. [79], where the connection between striation lines and fatigue crack growth rate are demonstrated, as depicted in Fig. 26.

In Fig. 26-a, SEM pictures have been utilized to examine the correlation between striation space and fatigue crack propagation rate. The figure illustrates when the crack is extended by 4 mm ($\Delta a = 4$ mm), the measured striation spacing is 4.66. This finding indicates a distinct fatigue crack growth rate at that particular location which equals 4.66 μm per cycle. Upon comparing Fig. 26-a to d, it becomes evident which with the gradual increase in the fatigue crack growth rate, da/dN, the distance between the striation lines also increases. It should be mentioned that when the fatigue crack growth rate is very low, the striation marks may not be sufficiently recognizable under the SEM microscope. Also, when the crack growth rate is very high, the fiber imprint surfaces are very rugged and fragmented, and as a result, the striation lines will not be visible. In general, in order to observe the striation lines, a high skill of the operator is required. In some cases, in order to observe better, the sample holder should be rotated 45° in relation to the SEM electron beam.

7.5. Fracture surface as an indication of the energy release rate

Fractography images show a clear link between the release rate of fracture energy and the roughness of the fracture surface, as well as the

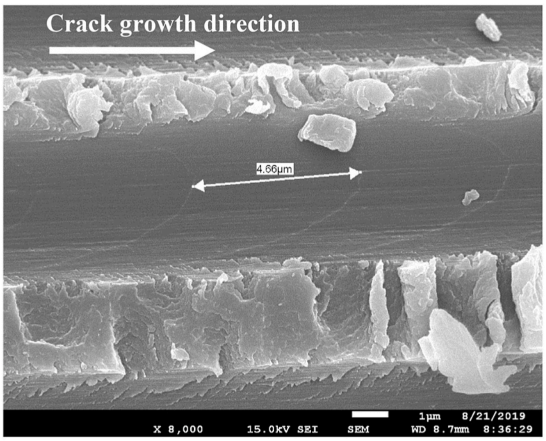

a) *da/dN* = 2.06e-6 m/cycle & Δ*a*=4 mm& *N*=4950

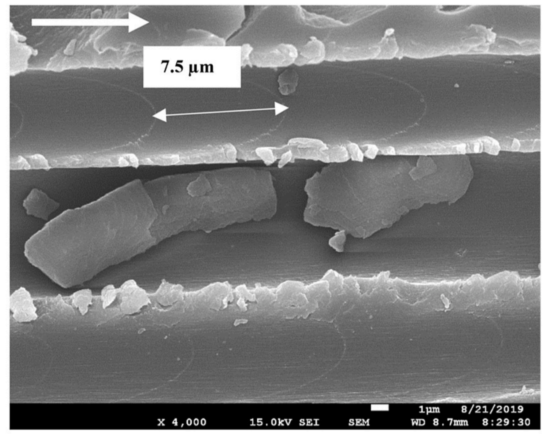

b) *da/dN* = 6.73e-6 m/cycle & Δ*a*=6 mm& *N*=5380

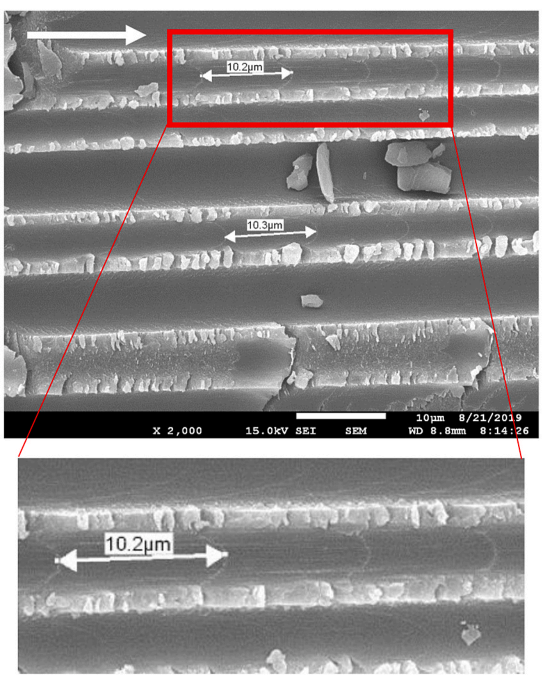

c) *da/dN* = 9.62e-6 m/cycle & Δ*a*=8 mm& *N*=5590

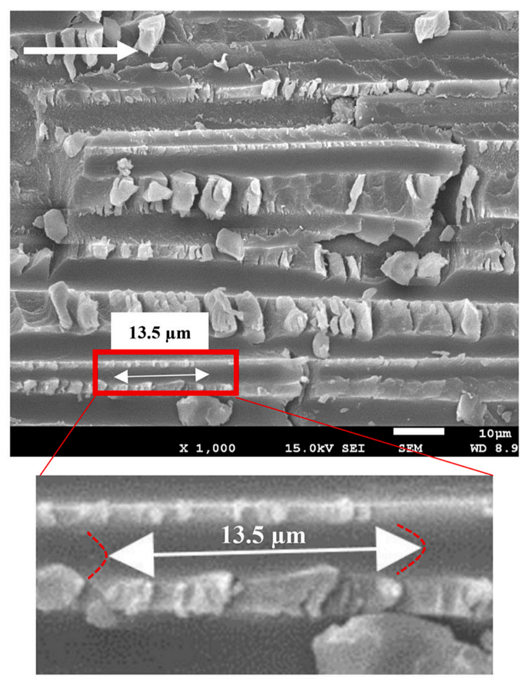

d) *da/dN* = 1e-5 m/cycle & Δ*a*=10 mm& *N*=5700

Fig. 26. The relationship between striation lines and the rate of mode II fatigue crack growth in CFRP laminates [79].

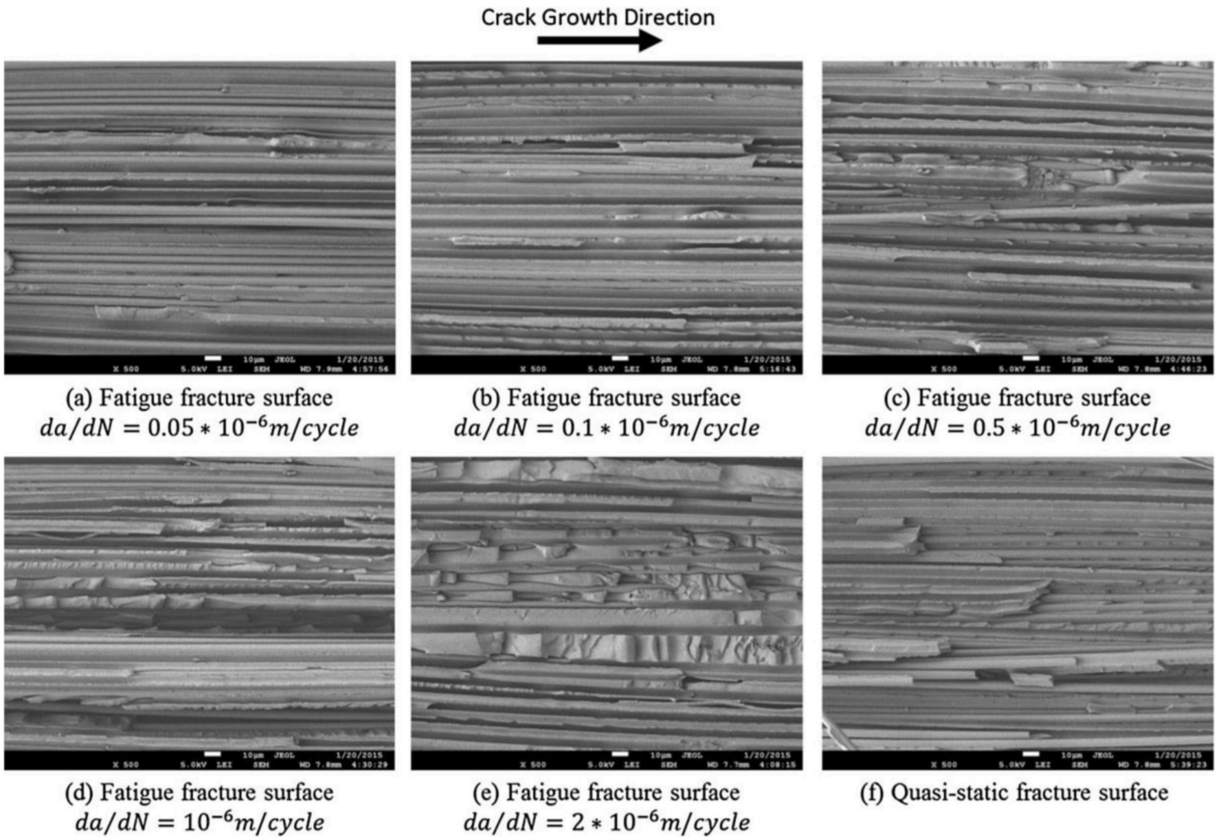

Fig. 27. The fractography images can be shows the energy release rate [87].

displayed damage characteristics. This correlation is depicted in Fig. 27 which CFRP specimens have been test under mode I fatigue loading condition. This figure effectively illustrates the progression of fracture surfaces, beginning with a smoother surface in Fig. 27 (a) at lower crack growth rates and gradually incorporating an increasing number of fractography features. Finally, in the static test, due to the sudden and rapid growth of the crack, the delamination surfaces have the most roughness as shown in Fig. 27 (f). Fig. 27 illustrates that at low crack growth rates, the fatigue failure surfaces are entirely smooth and flat. As the fatigue crack growth rate increases, along with the corresponding rise in strain energy released rate, the fracture surfaces become rougher and various damage mechanisms, including cusps and fiber breakage are activated. Accordingly, the micrograph of fracture surfaces, reflect the amount of strain energy released during delamination propagation, providing valuable insights into the intensity of loading and impact during catastrophic events. Furthermore, based on the fractographic images, it can be concluded which of the damage features played the most significant role in energy dissipation. For instance, in quasi-static tests, decohesion processes linked to fiber breakage and matrix cracking emerge as the predominant mechanisms for energy absorption.

Fig. 28 illustrates the concurrent relationship between the strain energy release rate (dU/dN), fatigue crack growth rate (da/dN), and fractographic damage features on delamination surfaces. This figure relates to mode I fatigue loading conducted on AS4/8552 carbon/epoxy specimens provided by the authors. The carbon/epoxy specimens, measuring 190 *25 *4.5 mm^3, were prepared for this study. Initial pre-cracks were induced in the samples, which were then subjected to mode I fatigue loading following the standard ASTM D6115. The specimens underwent sinusoidal cyclic loading at a frequency of 3 Hz with a cyclic loading ratio of $R = 0.3$. Further details regarding the methodology and approach for this figure can be found in Ref. [67]. Following fatigue testing and substantial crack propagation, SEM pictures were prepared at various distances from the initial pre-crack (Δa).

Essentially, the energy released during crack propagation reflects the specific damage features observed on the delamination surface. The strain energy release rate values under fatigue and quasi-static loading conditions exhibit correlation. Fatigue loading, with lower da/dN values, establishes the lower boundary, associated with minimal energy released and smoother fracture surfaces. Conversely, quasi-static fractures, characterized by matrix cleavage and fiber breakage, define the upper limit with the highest energy released rate.

8. Conclusion

This comprehensive review paper focused on various damage mechanisms and associated phenomena that appear during delamination within composite materials. Delamination can primarily appear in mode I and mode II loading scenarios, occurring under both static and fatigue loading conditions. Notably, the micro -mechanisms of damage diverge significantly between these conditions. In this study, the initial exploration focused on various phenomena occurring during delamination, including fiber bridging and resin enrichment at the initial crack tip. In the following, a comprehensive examination of primary damage mechanisms dominated by delamination, such as fiber breakage, fiber-matrix debonding, matrix cracking, and associated damage features, has been conducted. This analysis was based on an extensive review of the literature, utilizing fractography method. The study's findings showed that a thorough fractography analysis of fracture surfaces and an examination of damage mechanisms and related features provide valuable outputs from loading conditions of composite structures. For instance, considering scarps and river lines allows for the determination of the global crack growth direction. Additionally, studying the orientation of cusps enables the identification of shear stress direction and the crack growth direction during delamination in mode II loading. Furthermore, the fatigue crack growth rate (da/dN) can be calculated through the analysis of striation marks distances. These findings offer

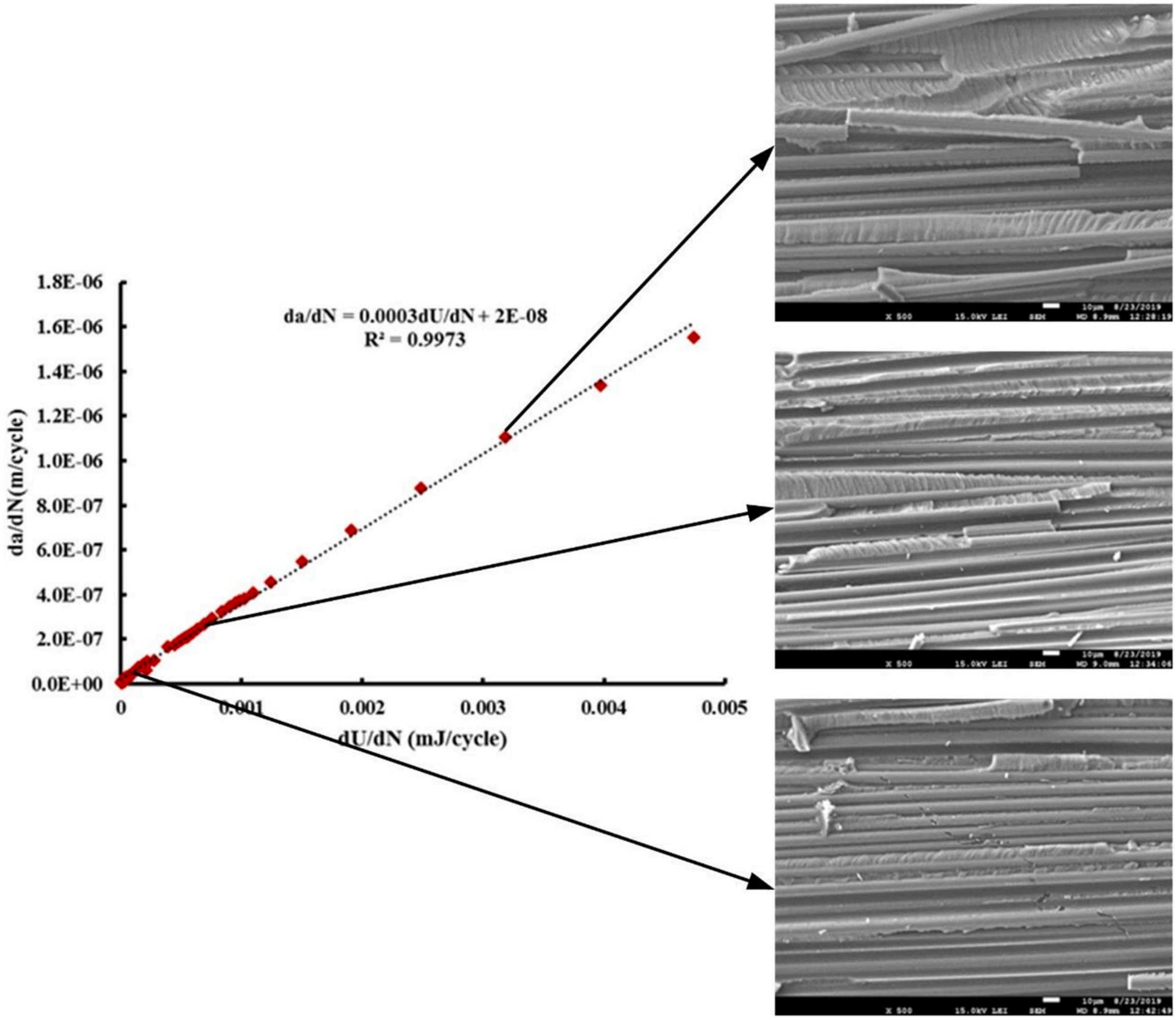

Fig. 28. The correlation between damage surface and energy dissipation in mode I fatigue conditions.

valuable insights for designing delamination-resistant composites. Moreover, they could aid in identifying the root causes of catastrophic failures in tragic events.

CRediT authorship contribution statement

Reza Mohammadi: Writing – review & editing, Writing – original draft, Methodology, Conceptualization. **Maher Assaad:** Writing – review & editing, Investigation, Conceptualization. **Ahmed Imran:** Writing – original draft, Resources, Data curation. **Mohammad Fotouhi:** Writing – review & editing, Supervision, Methodology, Funding acquisition, Conceptualization.

Declaration of competing interest

The authors declare that they have no known competing financial interests or personal relationships that could have appeared to influence the work reported in this paper.

Data availability

No data was used for the research described in the article.

Acknowledgements

This research received partial funding from Ajman University (2022-IRG-ENIT-1) and the UK Engineering and Physical Sciences Research Council (EP/V009451/1). The data essential for supporting the conclusions are presented within the paper.

References

[1] T. Zhu, Z. Ren, J. Xu, L. Shen, C. Xiao, C. Zhang, et al., Damage evolution model and failure mechanism of continuous carbon fiber-reinforced thermoplastic resin matrix composite materials, Compos. Sci. Technol. 244 (2023) 110300.
[2] J.R. Shao, N. Liu, Z.J. Zheng, Y. Yang, Elastic-plastic progressive damage model and low-velocity impact failure mechanism of composite materials, Mater. Today Commun. 31 (2022) 103685.
[3] M. Ahangar, M. Saeedifar, The effect of plasma treatment on the mode II interlaminar fracture toughness of Glass/Epoxy laminates, Theor. Appl. Fract. Mech. 127 (2023) 104093.
[4] M. Saeedifar, J. Mansvelder, R. Mohammadi, D. Zarouchas, Using passive and active acoustic methods for impact damage assessment of composite structures, Compos. Struct. 226 (2019) 111252.
[5] W. Harizi, S. Chaki, G. Bourse, M. Ourak, Damage mechanisms assessment of Glass Fiber-Reinforced Polymer (GFRP) composites using multivariable analysis methods applied to acoustic emission data, Compos. Struct. 289 (2022) 115470.
[6] C.V. Opelt, G.M. Cândido, M.C. Rezende, Fractographic study of damage mechanisms in fiber reinforced polymer composites submitted to uniaxial compression, Eng. Fail. Anal. 92 (2018) 520–527.
[7] R. Mohammadi, M.A. Najafabadi, M. Saeedifar, J. Yousefi, G. Minak, Correlation of acoustic emission with finite element predicted damages in open-hole tensile laminated composites, Compos. B Eng. 108 (2017) 427–435.

[8] W. Li, Y. Liu, P. Jiang, F. Guo, J. Cheng, Study on delamination damage of CFRP laminates based on acoustic emission and micro visualization, Materials 15 (2022).
[9] M. Saeedifar, M. Ahmadi Najafabadi, H. Hoseyni, R. Mohammadi, Investigation of initiation and evolution of delamination in glass/epoxy laminated composites using acoustic emission method, Amirkabir J. Mech. Eng. 48 (2016) 411–422.
[10] Z. Liu, L. Yan, Z. Wu, J. Zhou, H. Wei, S. Zhang, et al., Progressive damage analysis and experiments of open-hole composite laminates subjected to compression loads, Eng. Fail. Anal. 151 (2023) 107379.
[11] Y. Li, B. Wang, L. Zhou, Study on the effect of delamination defects on the mechanical properties of CFRP composites, Eng. Fail. Anal. 153 (2023) 107576.
[12] J. Yousefi, R. Mohamadi, M. Saeedifar, M. Ahmadi, H. Hosseini-Toudeshky, Delamination characterization in composite laminates using acoustic emission features, micro visualization and finite element modeling, J. Compos. Mater. 50 (2015) 3133–3145.
[13] J. Bonhomme, A. Argüelles, J. Viña, I. Viña, Fractography and failure mechanisms in static mode I and mode II delamination testing of unidirectional carbon reinforced composites, Polym. Test. 28 (2009) 612–617.
[14] M. Saeedifar, H. Hosseini Toudeshky, The effect of interlaminar and intralaminar damage mechanisms on the quasi-static indentation strength of composite laminates, Appl. Compos. Mater. 30 (2023) 871–886.
[15] L. Yao, M. Chuai, J. Liu, L. Guo, X. Chen, R.C. Alderliesten, et al., Fatigue delamination behavior in composite laminates at different stress ratios and temperatures, Int. J. Fatig. 175 (2023) 107830.
[16] V. Moorthy, K. Marappan, Experimental study on delamination identification in tapered laminated composite plates using damage detection models, Compos. Struct. 323 (2023) 117494.
[17] L. Yao, M. Chuai, H. Li, X. Chen, D. Quan, R.C. Alderliesten, et al., Temperature effects on fatigue delamination behavior in thermoset composite laminates, Eng. Fract. Mech. 295 (2024) 109799.
[18] P. Jadhav, Modeling of mode 1 delamination behavior in laminated composite structures for aerospace applications, Mater. Today: Proc. 82 (2023) 61–67.
[19] C. Liu, Y. Gong, Y. Gong, W. Li, Z. Liu, N. Hu, Mode II fatigue delamination behaviour of composite multidirectional laminates and the stress ratio effect, Eng. Fract. Mech. 264 (2022) 108321.
[20] A. Ghadirdokht, M. Heidari-Rarani, Delamination R-curve behavior of curved composite laminates, Compos. B Eng. 175 (2019) 107139.
[21] D. Xu, P.F. Liu, Z.P. Chen, J.G. Li, J.X. Leng, R.H. Zhu, et al., Delamination analysis of carbon fiber/epoxy composite laminates under different loading rates using acoustic emission, J. Fail. Anal. Prev. 19 (2019) 1034–1042.
[22] M. Fotouhi, S. Sadeghi, M. Jalalvand, M. Ahmadi, Analysis of the damage mechanisms in mixed-mode delamination of laminated composites using acoustic emission data clustering, J. Thermoplast. Compos. Mater. 30 (2015) 318–340.
[23] D. Quan, N. Murphy, A. Ivanković, G. Zhao, R. Alderliesten, Fatigue delamination behaviour of carbon fibre/epoxy composites interleaved with thermoplastic veils, Compos. Struct. 281 (2022) 114903.
[24] U. Kemiklioğlu, Mechanical and morphological investigation of laminated composite polymers depending on increasing vibration cycle, Int. J. Polym. Anal. Char. 1 (2023) 726–733.
[25] M.S.S. Bathusha, I.U. Din, R. Umer, K.A. Khan, In-situ monitoring of crack growth and fracture behavior in composite laminates using embedded sensors of rGO coated fabrics and GnP paper, Sensor Actuator Phys. 365 (2024) 114850.
[26] S.I.B. Syed Abdullah, S.K. Bokti, K.J. Wong, M. Johar, W.W.F. Chong, Y. Dong, Mode II and mode III delamination of carbon fiber/epoxy composite laminates subjected to a four-point bending mechanism, Compos. B Eng. 270 (2024) 111110.
[27] I.S. Raju, T.K. O'Brien, 1 - fracture mechanics concepts, stress fields, strain energy release rates, delamination initiation and growth criteria, in: S. Sridharan (Ed.), Delamination Behaviour of Composites, Woodhead Publishing, 2008, pp. 3–27.
[28] M. Saeedifar, M.A. Najafabadi, D. Zarouchas, H.H. Toudeshky, M. Jalalvand, Barely visible impact damage assessment in laminated composites using acoustic emission, Compos. B Eng. 152 (2018) 180–192.
[29] K. Karthik, A. Belay Teferi, R. Sathish, A.G. MohanDas Gandhi, S.N. Padhi, S. Boopathi, et al., Analysis of delamination and its effect on polymer matrix composites, Mater. Today: Proc. (2023).
[30] N. Zarif Karimi, H. Heidary, G. Minak, M. Ahmadi, Effect of the drilling process on the compression behavior of glass/epoxy laminates, Compos. Struct. 98 (2013) 59–68.
[31] S. Sridharan, Y. Li, S. El-Sayed, 21 - delamination failure under compression of composite laminates and sandwich structures, in: S. Sridharan (Ed.), Delamination Behaviour of Composites, Woodhead Publishing, 2008, pp. 618–649.
[32] S. Sridharan, Delamination Behaviour of Composites, Elsevier Science, 2008.
[33] A. Tabatabaeian, B. Jerkovic, P. Harrison, E. Marchiori, M. Fotouhi, Barely visible impact damage detection in composite structures using deep learning networks with varying complexities, Compos. B Eng. 264 (2023) 110907.
[34] S. Fotouhi, M. Jalalvand, M.R. Wisnom, M. Fotouhi, Smart hybrid composite sensor technology to enhance the detection of low energy impact damage in composite structures, Compos. Appl. Sci. Manuf. 172 (2023) 107595.
[35] M.N. Saleh, H.M. El-Dessouky, M. Saeedifar, S.T. De Freitas, R.J. Scaife, D. Zarouchas, Compression after multiple low velocity impacts of NCF, 2D and 3D woven composites, Compos. Appl. Sci. Manuf. 125 (2019) 105576.
[36] ASTM D 5528-13, Standard Test Method for Mode I Interlaminar Fracture Toughness of Unidirectional Fiber-Reinforced Polymer Matrix Composites, ASTM International, West Conshohocken, PA, 2022, p. 2022.
[37] ASTM D7905, Standard Test Method for Determination of the Mode II Interlaminar Fracture Toughness of Unidirectional Fiber-Reinforced Polymer Matrix Composites, ASTM International, West Conshohocken, PA, 2019, p. 2019.
[38] ASTM D 6671-01, Standards Test Method for Mixed Mode I-Mode II Interlaminar Fracture Toughness of Unidirectional Fiber Reinforced Polymer Matrix Composites, ASTM International, West Conshohocken, PA, 2022, p. 2022.
[39] ASTM D6115-97, Standard Test Method for Mode I Fatigue Delamination Growth Onset of Unidirectional Fiber-Reinforced Polymer Matrix Composites, ASTM International, West Conshohocken, PA, 2019, p. 2019.
[40] R. Mohammadi, M. Saeedifar, H.H. Toudeshky, M.A. Najafabadi, M. Fotouhi, Prediction of delamination growth in carbon/epoxy composites using a novel acoustic emission-based approach, J. Reinforc. Plast. Compos. 34 (2015) 868–878.
[41] X. Li, S. Shonkwiler, S. McMains, Detection of resin-rich areas for statistical analysis of fiber-reinforced polymer composites, Compos. B Eng. 225 (2021) 109252.
[42] H. Ahmadian, M. Yang, S. Soghrati, Effect of resin-rich zones on the failure response of carbon fiber reinforced polymers, Int. J. Solid Struct. 188–189 (2020) 74–87.
[43] F. Sacchetti, W.J.B. Grouve, L.L. Warnet, I.F. Villegas, Effect of resin-rich bond line thickness and fibre migration on the toughness of unidirectional Carbon/PEEK joints, Compos. Appl. Sci. Manuf. 109 (2018) 197–206.
[44] H. Ghayoor, C.C. Marsden, S.V. Hoa, A.R. Melro, Numerical analysis of resin-rich areas and their effects on failure initiation of composites, Compos. Appl. Sci. Manuf. 117 (2019) 125–133.
[45] S. Yamashita, Y. Nakashima, J. Takahashi, K. Kawabe, T. Murakami, Volume resistivity of ultra-thin chopped carbon fiber tape reinforced thermoplastics, Compos. Appl. Sci. Manuf. 90 (2016) 598–605.
[46] S. Hassan, Chapter 4, 2015.
[47] R. Mohammadi, M.A. Najafabadi, H. Saghafi, D. Zarouchas, Mode-II fatigue response of AS4/8552 carbon/epoxy composite laminates interleaved by electrospun nanofibers, Thin-Walled Struct. 154 (2020) 106811.
[48] P. Davies, W. Cantwell, H.H. Kausch, Measurement of initiation values of GIC in IM6/PEEK composites, Compos. Sci. Technol. 35 (1989) 301–313.
[49] P. Davies, C. Moulin, H.H. Kausch, M. Fischer, Measurement of GIc and GIIc in carbon/epoxy composites, Compos. Sci. Technol. 39 (1990) 193–205.
[50] R. Mohammadi, R. Akrami, M. Assaad, M. Nasor, A. Imran, M. Fotouhi, Polysulfone nanofiber-modified composite laminates: investigation of mode-I fatigue behavior and damage mechanisms, Theor. Appl. Fract. Mech. 127 (2023) 104078.
[51] R. Khan, Fiber bridging in composite laminates: a literature review, Compos. Struct. 229 (2019) 111418.
[52] L. Yao, Y. Sun, L. Guo, X. Lyu, M. Zhao, L. Jia, et al., Mode I fatigue delamination growth with fibre bridging in multidirectional composite laminates, Eng. Fract. Mech. 189 (2018) 221–231.
[53] J. Meng, H. Lei, Y. Li, Y. Ma, H. Yang, P. Wang, et al., Mode I fracture toughness with fiber bridging of unidirectional composite laminates under cryogenic temperature, Compos. Sci. Technol. 246 (2024) 110386.
[54] L. Yao, Y. Sun, L. Guo, M. Zhao, L. Jia, R.C. Alderliesten, et al., A modified Paris relation for fatigue delamination with fibre bridging in composite laminates, Compos. Struct. 176 (2017) 556–564.
[55] J. Cao, J. Gu, Z. Dang, C. Zhang, On temperature-dependent fiber bridging in mode I delamination of unidirectional composite laminates, Compos. Appl. Sci. Manuf. 171 (2023) 107581.
[56] C. Fu, X. Wang, Simulating delamination in composite laminates involving large scale fiber bridging based on the mixed-mode three-linear cohesive zone model, Theor. Appl. Fract. Mech. 117 (2022) 103164.
[57] Y. Gong, L. Zhao, J. Zhang, N. Hu, Crack closure in the fatigue delamination of composite multidirectional DCB laminates with large-scale fiber bridging, Compos. Struct. 244 (2020) 112220.
[58] L. Yao, Y. Sun, L. Guo, R.C. Alderliesten, R. Benedictus, M. Zhao, et al., Fibre bridging effect on the Paris relation of mode I fatigue delamination in composite laminates with different thicknesses, Int. J. Fatig. 103 (2017) 196–206.
[59] L. Yao, Y. Sun, M. Zhao, R.C. Alderliesten, R. Benedictus, Stress ratio dependence of fibre bridging significance in mode I fatigue delamination growth of composite laminates, Compos. Appl. Sci. Manuf. 95 (2017) 65–74.
[60] R.C. Alderliesten, A.J. Brunner, J.A. Pascoe, Cyclic fatigue fracture of composites: what has testing revealed about the physics of the processes so far? Eng. Fract. Mech. 203 (2018) 186–196.
[61] Y. Zhou, Y. Cao, J. Cao, C. Zhang, J. Li, Z. Wang, Fracture toughness and fiber bridging mechanism for mode-I interlaminar failure of spread-tow woven composites, Eng. Fract. Mech. 298 (2024) 109957.
[62] M.R. Hosseini, F. Taheri-Behrooz, M. Salamat-talab, Mode I interlaminar fracture toughness of woven glass/epoxy composites with mat layers at delamination interface, Polym. Test. 78 (2019) 105943.
[63] A. Gholizadeh, M.A. Najafabadi, H. Saghafi, R. Mohammadi, Considering damages to open-holed composite laminates modified by nanofibers under the three-point bending test, Polym. Test. 70 (2018) 363–377.
[64] E.H. Saidane, D. Scida, M.-J. Pac, R. Ayad, Mode-I interlaminar fracture toughness of flax, glass and hybrid flax-glass fibre woven composites: failure mechanism evaluation using acoustic emission analysis, Polym. Test. 75 (2019) 246–253.
[65] M.T. Bashar, U. Sundararaj, P. Mertiny, Mode-I interlaminar fracture behaviour of nanoparticle modified epoxy/basalt fibre-reinforced laminates, Polym. Test. 32 (2013) 402–412.
[66] M. Saeedifar, M. Ahmadi Najafabadi, K. Mohammadi, M. Fotouhi, H. Hosseini Toudeshky, R. Mohammadi, Acoustic emission-based methodology to evaluate delamination crack growth under quasi-static and fatigue loading conditions, J. Nondestr. Eval. 37 (2017) 1.
[67] R. Mohammadi, M.A. Najafabadi, H. Saghafi, D. Zarouchas, Fracture and fatigue behavior of carbon/epoxy laminates modified by nanofibers, Compos. Appl. Sci. Manuf. 137 (2020) 106015.

[68] C. Blondeau, G.A. Pappas, J. Botsis, Crack propagation in CFRP laminates under mode I monotonic and fatigue loads: a methodological study, Compos. Struct. 256 (2021) 113002.

[69] M.J. Hiley, Delamination between multi-directional ply interfaces in carbon-epoxy composites under static and fatigue loading, in: J.G. Williams, A. Pavan (Eds.), European Structural Integrity Society, Elsevier, 2000, pp. 61–72.

[70] S.L. Ogin, P. Brøndsted, J. Zangenberg, 1 - composite materials: constituents, architecture, and generic damage, in: R. Talreja, J. Varna (Eds.), Modeling Damage, Fatigue and Failure of Composite Materials, Woodhead Publishing, 2016, pp. 3–23.

[71] L. Yao, H. Cui, Y. Sun, L. Guo, X. Chen, M. Zhao, et al., Fibre-bridged fatigue delamination in multidirectional composite laminates, Compos. Appl. Sci. Manuf. 115 (2018) 175–186.

[72] X. Li, R. Benedictus, D. Zarouchas, Analysis of stochastic matrix crack evolution in CFRP cross-ply laminates under fatigue loading, Eng. Fail. Anal. 150 (2023) 107277.

[73] E. Greenhalgh, Failure Analysis and Fractography of Polymer Composites, Elsevier, 2009.

[74] K.N. Shivakumar, R. Panduranga, J. Skujins, S. Miller, Assessment of mode-II fracture tests for unidirectional fiber reinforced composite laminates, J. Reinforc. Plast. Compos. 34 (2015) 1905–1925.

[75] M.J. Hiley, Fractographic study of static and fatigue failures in polymer composites, Plast., Rubber Compos. 28 (1999) 210–227.

[76] X. Gao, M. Umair, Y. Nawab, Z. Latif, S. Ahmad, A. Siddique, et al., Mode I fatigue of fibre reinforced polymeric composites: a review, Polymers 14 (2022) 214558.

[77] R.C. Alderliesten, Critical review on the assessment of fatigue and fracture in composite materials and structures, Eng. Fail. Anal. 35 (2013) 370–379.

[78] R. Mohammadi, M. Ahmadi Najafabadi, H. Saghafi, M. Saeedifar, D. Zarouchas, A quantitative assessment of the damage mechanisms of CFRP laminates interleaved by PA66 electrospun nanofibers using acoustic emission, Compos. Struct. 258 (2021) 113395.

[79] R. Mohammadi, M.A. Najafabadi, H. Saghafi, M. Saeedifar, D. Zarouchas, The effect of mode II fatigue crack growth rate on the fractographic features of CFRP composite laminates: an acoustic emission and scanning electron microscopy analysis, Eng. Fract. Mech. 241 (2021) 107408.

[80] E.S. Greenhalgh, C. Rogers, P. Robinson, Fractographic observations on delamination growth and the subsequent migration through the laminate, Compos. Sci. Technol. 69 (2009) 2345–2351.

[81] L. Longbiao, Relationship between hysteresis dissipated energy and temperature rising in fiber-reinforced ceramic-matrix composites under cyclic loading, Appl. Compos. Mater. 23 (2016) 337–355.

[82] B. Sjögren, L. Asp, E. Greenhalgh, M.J. Hiley, Interlaminar Crack Propagation in CFRP: Effects of Temperature and Loading Conditions on Fracture Morphology and Toughness, ASTM Special Technical Publication, 2002, pp. 235–252.

[83] M.J. Hiley, Fractographic study of static and fatigue failures in polymer composites, Plast., Rubber Compos. 28 (1999) 210–227.

[84] E. Greenhalgh, Failure Analysis and Fractography of Polymer Composites, Woodhead Publishing Series in Composites Science and Engineering, 2009, pp. 1–595.

[85] Fractography of composites, in: S. Lampman (Ed.), Characterization and Failure Analysis of Plastics, ASM International, 2003, p. 1.

[86] A. McEvily, H. Matsunaga, On Fatigue Striations, 2010.

[87] L. Amaral, L. Yao, R. Alderliesten, R. Benedictus, The relation between the strain energy release in fatigue and quasi-static crack growth, Eng. Fract. Mech. 145 (2015) 86–97.